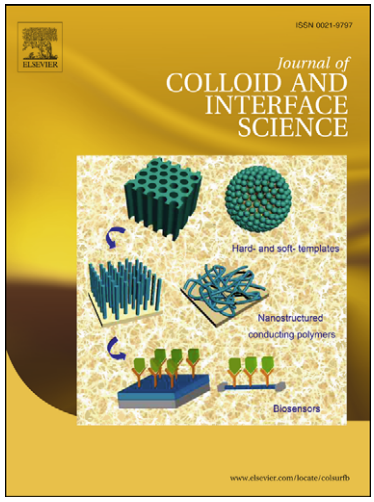


# Syntheses of Complex Mesoporous Silicas Using Mixtures of Nonionic Block Copolymer Surfactants: Understanding Formation of Different Structures Using Solubility Parameters

Lan Chen, Ju Xu, Wen-Hua Zhang, Justin D Holmes, Michael A. Morris

PII: S0021-9797(10)01094-5
DOI: 10.1016/j.jcis.2010.09.043
Reference: YJCIS 16216

To appear in: *Journal of Colloid and Interface Science*

Received Date: 31 March 2010
Accepted Date: 15 September 2010

Please cite this article as: L. Chen, J. Xu, W-H. Zhang, J.D. Holmes, M.A. Morris, Syntheses of Complex Mesoporous Silicas Using Mixtures of Nonionic Block Copolymer Surfactants: Understanding Formation of Different Structures Using Solubility Parameters, *Journal of Colloid and Interface Science* (2010), doi: 10.1016/j.jcis.2010.09.043

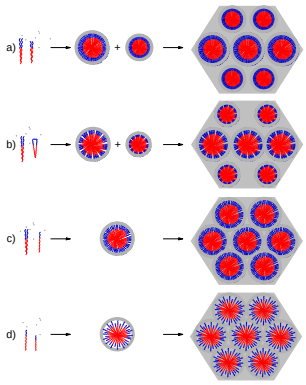


A polymeric co-surfactant can form different mesoporous structure upon the packing ability of the both member components in the presence of silicate species.

# Syntheses of Complex Mesoporous Silicas Using Mixtures of Nonionic Block Copolymer Surfactants: Understanding Formation of Different Structures Using Solubility Parameters

Lan Chen[a,*], Ju Xu[a], Wen-Hua Zhang[a], Justin D Holmes[a,b] and Michael A. Morris[a,b,*]

[a] Materials Section and Supercritical Centre, Department of Chemistry, University College Cork, Cork, Ireland

[b] Centre for Research on Adaptive Nanostructures and Nanodevices (CRANN), Trinity College Dublin, Dublin 2, Ireland

Email: lan.chen@ucc.ie; m.morris@ucc.ie

**Abstract**

The use of block copolymer (BCP) nonionic surfactant mixtures (including Pluronic, Brij and Tetronic types) as templates for synthesizing porous silica materials of mixed pore sizes is explored here. These systems have important applications because combinations of pore sizes can allow rapid access of reactants (via large pores) whilst providing the very high surface area of small pores for higher reaction rates or size selectivity. Examples of the materials prepared here include pore size bimodal hexagonal *p6mm* channel structures and cubic *Im3m* cage structures. It is shown here that the chemical similarity, as indicated by the solubility parameter, of the surfactants is an important factor in determining the pore structure and size distribution (PSD) of the pores. Monomodal pore structures are usually obtained when the solubility parameters of the surfactants are similar and bimodal pore structures when the solubility parameters are reasonably different. When the interaction parameter is very high disordered porous systems are formed. Ternary co-surfactant systems, e.g. P123-25R4-P65, can also yield highly ordered bimodal mesoporous silica with a hexagonal structure.

Keywords: Mesoporous, silica, synthesis, packing ability, co-surfactant

## 1. Introduction

The nonionic BCP surfactants with one or more alkylene oxide blocks are important families of surfactants widely used in the syntheses of mesoporous materials due to their low-cost, good aqueous solubility, non-toxicity and ease of de-templating [1-15]. The water solubility of these polymers derives from the association of water molecules with the alkylene oxide moieties through hydrogen bonding. Solubility increases in acid solutions because of the additional association of $H^+$ ions with the alkylene oxygen atoms [2]. For the Tetronic and Pluronic systems that largely comprise of poly(ethylene oxide) (PEO) and poly(proplene oxide) (PPO) blocks (as described below), the PEO block is considerably more hydrophilic than the PPO chain because of this hydrogen ion association [2]. As a consequence, in polar solvents these blocks can confer a spatial configuration difference which results in organized micelle arrangements which can be used to 'template' or structurally direct the condensation of inorganic species to yield lamellar, cubic and hexagonal mesostructures [2, 3, 5-7, 10-14, 16-19].

However, few papers have reported syntheses using more than one BCP surfactant despite the opportunities that surfactant mixing may offer for pore size engineering [20-22]. The possibility of combining surfactants to produce bimodal pore size distributions with large pores providing access to smaller pore systems for high surface area and possibly molecular size recognition would find many applications. Recently, various types of hierarchically (macro-micro [23, 24] macro-meso [3, 17], meso-micro [25, 26], and meso-meso [4, 27-35]) porous materials have been synthesized in an effort to prepare systems combining larger pores and smaller pores. In the case of Pluronic surfactant mixtures, early work results suggested that the resultant mesopore structures and pore sizes were a simple average of the individual surfactants [22, 36]. However, in a recent paper by us, it was shown that this was an overly simplistic model and even when similar types of Pluronic surfactants were combined, complex bimodal structures were obtained [37].

When surfactant mixtures template silica, there are various structural arrangements that can be formed, and these are described schematically in Figure 1. In Figure 1A the arrangement is a simple monomodal (i.e. uniform pore size through the material) hexagonal pore arrangement that might be formed when the surfactants form an ideal mixture within a single micelle. In Figure 1B, a bimodal arrangement is shown when two different surfactants are chemically different enough to either not mix or partially

mix but they are similar enough so as to allow structural packing of the pores in a well-defined arrangement. This was the most prevalent arrangement seen by us in earlier studies [37]. It should be noted, that the structure of these bimodal arrangements is difficult to prove because they will result in complex adsorption/desorption isotherms that are difficult to interpret. E.g. rather than forming discrete pores of uniform size it may be more likely that the pores consist of regions where the pores widen and contract as the micelle changes from one surfactant type to another. This is fully described elsewhere [37].

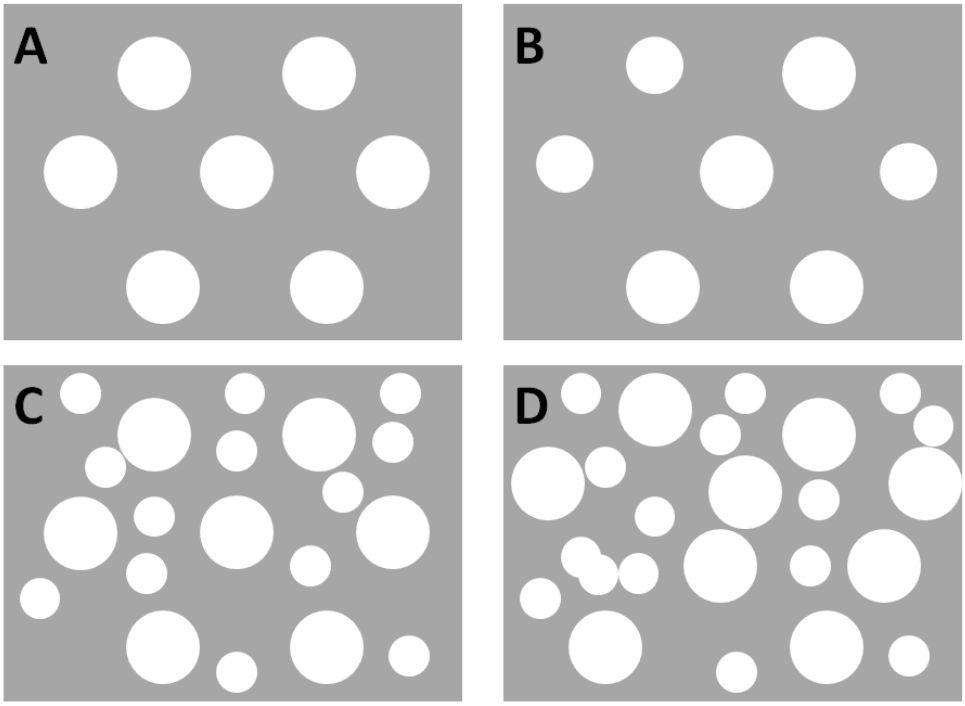


**Figure 1.** Schematic represent for interstitial and substitutional pore configuration of the dual pore/bimodal mesoporous systems.

Figure 1C shows a representation where there is no mixing of the surfactants and both are distributed in a bimodal arrangement but one of the pores is arranged in an ordered manner and one randomly. Finally, a disordered arrangement of separate pores are formed from surfactants where the micelles show no tendency to mix or pack into an ordered arrangement (Figure 1D). In this work, we extend the range of surfactants used previously [37] to examine if a general pattern for understanding how a mixture of surfactants might combine to yield porous structures.

## 2. Experimental

***2.1. Chemicals:*** The following materials used here were: B30, $C_{12}H_{25}(OCH_2CH_2)_4OH$ denoted $PE_{12}PEO_4$; B76, $C_{18}H_{37}(OCH_2CH_2)_{10}OH$ - $PE_{18}PEO_{10}$; Pluronic L121, $PEO_5PPO_{70}PEO_5$; Pluronic P65, $PEO_{20}PPO_{30}PEO_{20}$; Pluronic P123, $PEO_{20}PPO_{70}PEO_{20}$; Pluronic F127, $PEO_{106}PPO_{70}PEO_{106}$; Pluronic F88, $PEO_{100}PPO_{39}PEO_{100}$; Pluronic 25R4, $PPO_{19}PEO_{33}PPO_{19}$; Tetronic T701, $(PEO_2PPO_{14})_2NCH_2CH_2N(PPO_{14}PEO_2)_2$; Tetronic T90R4, $(PPO_{19}PEO_{16})_2NCH_2CH_2N(PEO_{16}PPO_{19})_2$; tetramethyl orthosilicate (TMOS) (Fluka); tetraethyl orthosilicate (TEOS) (Aldrich). All surfactants were sourced from Aldrich with exception of the Pluronics which were obtained from BASF.

The surfactants are classified in the following way. V-type surfactants have two PEO blocks (hydrophilic block) at the two ends and one central PPO block. Typical of these are Pluronic P123, F127, P65 and L121 *etc*. I-type surfactants have one polyethylene (PE) block (hydrophobic) and one PPO block (hydrophilic) e.g. Brij30 (B30) and Brij76 (B76). ∇-type surfactants have terminal PPO blocks (hydrophobic) and a central PEO block, e.g. Pluronic 25R4. Finally, X-type surfactants have four linear (PEO-b-PPO) di-blocks 'arms' radiating from a central amine molecule, such as Tetronic T90R4 and T701. A subscript number is also used to denote the relative length of the PPO (alkyl) block to PEO block. '1' means the molecule has larger PPO (alkyl) block while '2' refers to a molecule having a larger PEO block. E.g. Pluronic P123, P65, L121 belong to $V_1$ and Pluronic F127, F88 belong to $V_2$.

***2.2. Synthesis:*** The porous silicas were obtained via acid catalyzed hydrolysis-condensation using the surfactant mixtures. In Pluronic P123-derived syntheses, 0.17 mmol of Pluronic P123 was dissolved in 63 ml of water and 12 ml 37.5 wt % HCl solution under stirring at 40 °C for 1 hour. After addition of 0.17 mmol of the other copolymers into this solution, the mixture was stirred for another 4 hours at 40 °C (at room temperature (RT) for the F127 containing synthesis). Then 5 ml of TEOS was added drop wise into this solution and then stirred for a further 20 hours. Finally, the mixture was aged statically at 105 °C in a Teflon-lined autoclave for 48 hours.

The Pluronic F127-derived syntheses are similar to those of P123. 0.17 mmol of F127 copolymer was dissolved in 12 ml of 37.5 wt % HCl and 63 ml of water under stirring at RT until total dissolution. To this solution, 0.17 mmol of the co-surfactants

were added. After 2 h of stirring, 3.5 ml of TMOS was added in the solution and stirred for 10 h at RT again. The mixture was aged statically at RT for 60 h.

In the B76-derived syntheses, 0.17 mmol of B76 and the co-surfactants were dissolved in 12 ml of 37.5 wt% HCl solution and 63 ml of water respectively under stirring at RT. After 1.5 h, 3.5 ml of TMOS was syringed into the solution and stirred for 10 h. The resultant mixture was kept at RT statically for 48 h. For the B76, -F127 and -25R4 system, 0.323 mmol of B76 and 0.017 mmol of F127 and 25R4 were used as the co-surfactants and other conditions were maintained.

In the 90R4-derived syntheses, 0.17 mmol of Tetronic 90R4 and other nonionic surfactants were added into 1.6 M 75 ml of HCl solution (12 ml of 37.5 wt% HCl + 63 ml of $H_2O$) respectively under stirring at RT. After 3 h, 3.5 ml of TMOS was added into the above solution, with a further 20 h of stirring. The resultant mixture was aged statically at RT for 48 h.

All of the as-synthesized white solids were recovered by filtration and washed with distilled water 3~5 times and then air-dried at 105 °C overnight. The dried materials were then placed in an oven and calcined in air at 500 °C for 10 h.

***2.3. Analysis:*** Powder x-ray diffraction (XRD) patterns were recorded on a Phillips Xpert MPD diffractometer using Cu *Kα* radiation. Transmission electron micrographs (TEM) were collected on a JEM-2011 electron microscope operating at 200 kV. Powder samples were dispersed into ethanol and 1 or 2 drops of the solution were placed on a holey carbon film TEM grid and dried in ambient overnight. Nitrogen sorption isotherms at 77 K were measured using a Micromeritics Gemini 2375 volumetric analyzer. All samples were degassed under flowing nitrogen at 120 °C for 4 h prior to measurement.

## 3. Results

The following summarizes structural, microscopic and isothermal data collected from silica templated using various surfactant mixtures

### *3.1. $V_1$-type surfactant*

***a) $V_1$-$V_1$ co-surfactant:*** Low angle powder XRD patterns of calcined mesoporous silica (described as ORK-1 following previous work [37]) prepared by using equimolar combinations of P123-P65 and P123-L121 surfactant mixtures are described in Figure 2. Both routes produce similar materials showing 3 clear diffraction peaks in the $2\theta$ range from 0.8 to 2.0°. These features can be readily

assigned to an ordered mesoporous silica with *p6mm* hexagonal symmetry similar to SBA-15 [2] and the three peaks can be indexed as (100), (110) and (200) reflections. The lack of peak resolution of the higher angle features of the P123-P121 system compared to the P123-P65 system indicates a less well-ordered material. Unit cell parameters are 117.4 and 111.6 Å for P123-P65 and P123-L121 systems respectively. The $d_{100}$ (d-spacing of the (100) reflection) values are 101.5 and 97.0 Å for P123-P65 and P123-L121 respectively. Further evidence for the ordered arrangement of the P123-L121 and P123-P65 systems is provided by the TEM images presented in Figure 3. The micrographs show well-ordered hexagonal mesostructures viewed along the [001] and [110] directions and correspond to the well-known two-dimensional hexagonal mesopore structures [2, 8]. There is no evidence for disordered regions or the presence of any interstitial pores.

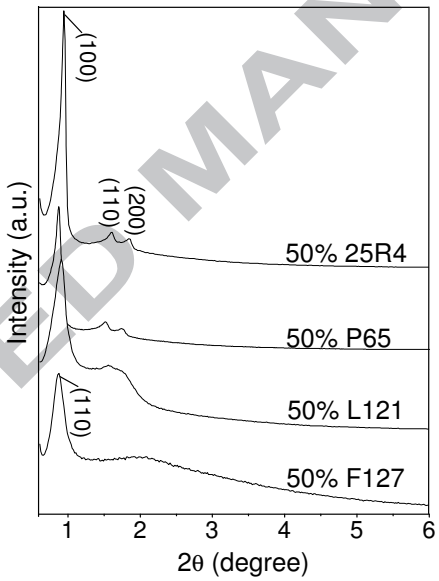


**Figure 2.** Powder x-ray diffraction patterns of Pluronic P123 (with an equimolar amount of other surfactants) derived mesoporous silica (after 500 °C calcination).

The $N_2$ sorption isotherms (Figure 4) for both P123-P65 and P123-L121 systems are type IV with clear hysteresis typical of ordered mesoporous materials and consistent with TEM and XRD data. Unusually, they show two well-defined steps in the adsorption and desorption curves between partial pressures $P/P_0$ of 0.4~0.6 (smaller steps) and 0.6~0.8 (larger steps). These steps result in pore size distributions (PSDs) (using Barrett–Joyner–Halanda (BJH) methodology) indicating a bimodal distribution of mesopore size for both surfactant mixtures. As described above and in

previous work [37], such isotherm/PSD data are hard to interpret but it is clear that different size pores are present (whether the pores are completely separately or vary in width through their length) in a bimodal distribution and the structure can be described as in Figure 1B. In both cases, the small pore sizes are similar at ca. 3.5 nm. The larger pore size of P123-L121 is about 6.8 nm and significantly greater than that of P123-P65 (~ 5.5 nm). It can be concluded for these systems that a bimodal structure is attained during silica synthesis. The P123-L121 system is significantly more disordered than P123-P65 as indicated by the width of the PSD as well as by the poorly resolved XRD data.

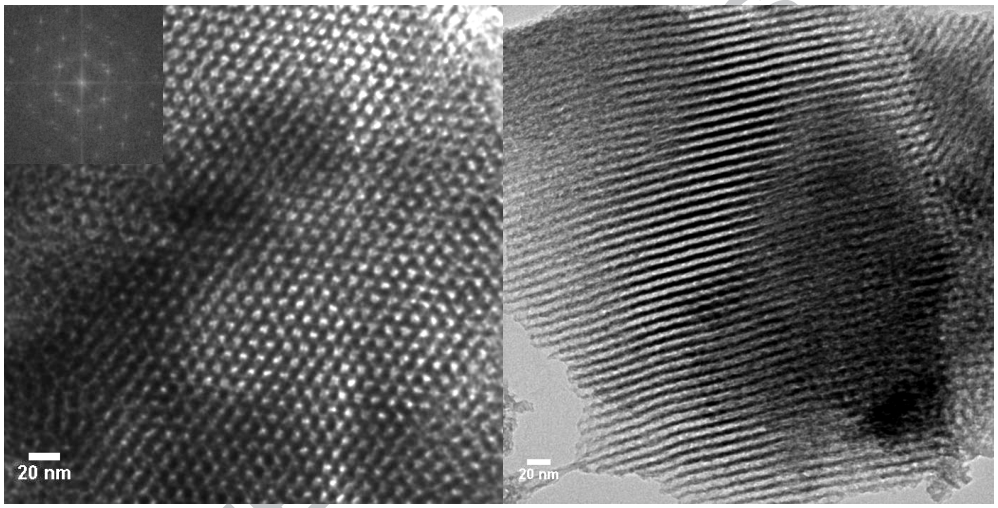


**Figure 3.** Transmission electron micrographs of a P123-P65 product calcined at 500 °C. Left is the view along the [001] direction and its corresponding Fourier Transformation (inset) and the view along the [110] direction (right).

***b) $V_1$- $V$co-surfactants:*** The products of this reaction are known as ORK-2. The low angle powder XRD pattern (Figure 2) of calcined mesoporous silica prepared from an equimolar mixture of P123 and 25R4 surfactants shows 3 clear diffraction peaks in the $2\theta$ range from 0.9 to 1.9°. The similarity of the data to that of P123-P65 allows assignment of the structure to a *p6mm* hexagonal lattice of parallel pores similar to SBA-15 [2]. The corresponding $d_{100}$ spacing was measured at 93.4 Å with a lattice parameter of 107.9 Å. It is clear that the structure consists of well packed mesopores with a parallel arrangement of hexagonally packed pores as evidenced by the TEM images presented in Figure 5.

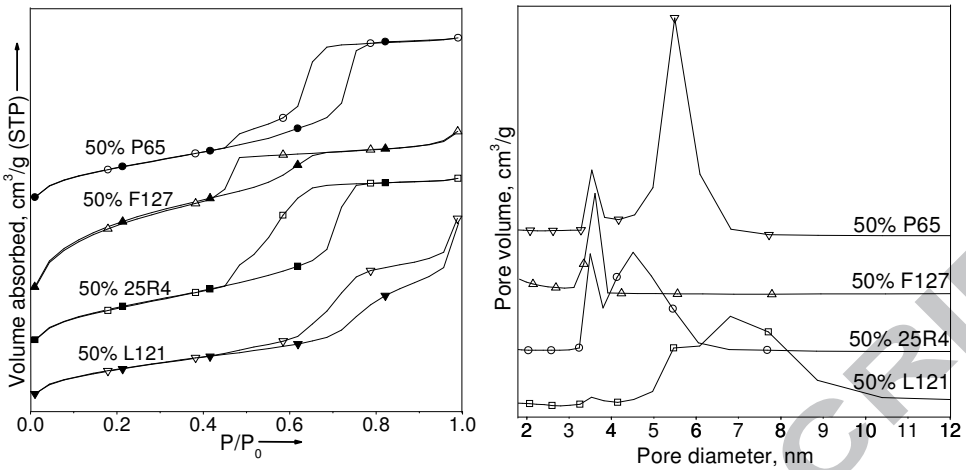


**Figure 4.** Nitrogen adsorption-desorption isotherms of Pluronic P123-derived products calcined at 500 °C (left) and (right) their corresponding pore-size distribution (PSD) curves (determined by Barrett-Joyner-Halenda (BJH) analysis on desorption branches of the isotherms). Solid symbols denote the adsorption branches while the open symbols indicate the desorption branch.

The $N_2$ sorption isotherm (Figure 4) of ORK-2 is again type IV and highly similar to the ORK-1 samples discussed. Two well-defined steps can be seen in the adsorption and desorption curves. These steps are subsequently translated (BJH method) into a PSD indicating a bimodal range of pore sizes. The small pore size is ca. 3.5 nm while the larger pore size is about 4.5 nm (desorption branch data). As for ORK-1 materials, it is possible to assign these data as being indicative of a bimodal distribution of pores within a highly well-ordered arrangement of pores as described in Figure 1B.

***c) $V_1$-$V_2$ co-surfactants:*** Mesoporous silica (ORK-3) was successfully synthesized by a co-surfactant mixture, P123-F127. XRD (Figure 2) reveals a single resolved diffraction peak at 0.87° 2$\theta$ with a second broad feature at about 2.1° 2$\theta$. The pattern is obviously indicative of a material with significantly less long-range order than previous samples. It is similar to the disordered cubic *Im3m* phases [8, 22] and the low angle diffraction peak indexed as a (110) reflection. The $d_{110}$ value is 101.7 Å with a corresponding unit cell parameter ($a=\sqrt{2}\,d$) of 143.8 Å. This is slightly smaller than that of pure F127 templating [8] and similar to co-surfactant templates by other authors [22]. The $N_2$ sorption isotherm (Figure 4) of ORK-3 is type IV with hysteresis and the calculated pore volume is 0.59 $cm^3\ g^{-1}$ is consistent with a porous material of this structure. The PSD data suggests a pore-size of 5.1 nm typical of

F127. Calculation of pore size from the desorption branch suggests an 'ink-bottle' structure with a neck size of about 3.5 nm [3, 22]. The width of the PSD is apparently quite narrow and suggests that some F127 derived pores exist in the material. On the basis of this data it is hard to see evidence for any strong interaction between the surfactants and it appears that no mixing has occurred with a disordered structure being formed.

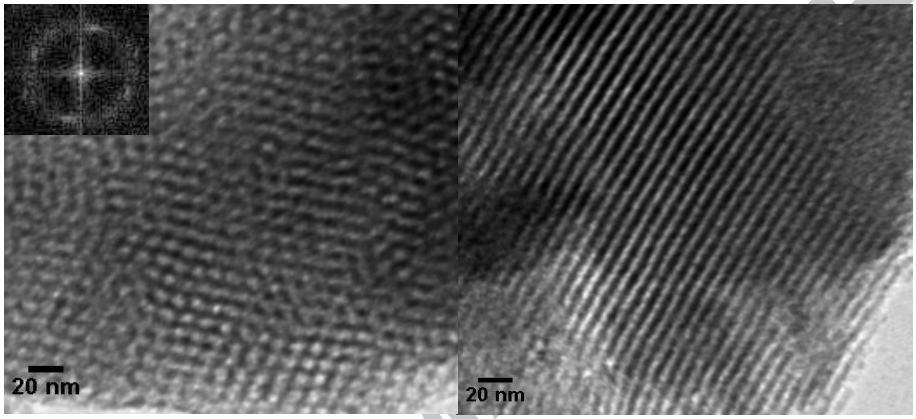


**Figure 5.** Transmission electron micrographs of a mesoporous silica templated by a equimolar mixture of P123 and 25R4 following calcination at 500 °C. Left, the view along the [001] direction and its corresponding Fourier Transformation inset and the view along the [110] direction (right).

Further evidence of the non-mixing of the surfactants can be seen by electron microscopy. Both TEM and SEM (Figure 6) images show the formation of relatively monodispersed mesoporous microspheres with diameter of around 0.5 μm. The spherical structure is typical of mesoporous sphere preparation where two different surfactant systems are used in combination to form the pores and define the particle morphology [38, 39]. Figure 6 also shows the disordered cubic pore structure viewed along the [110] direction.

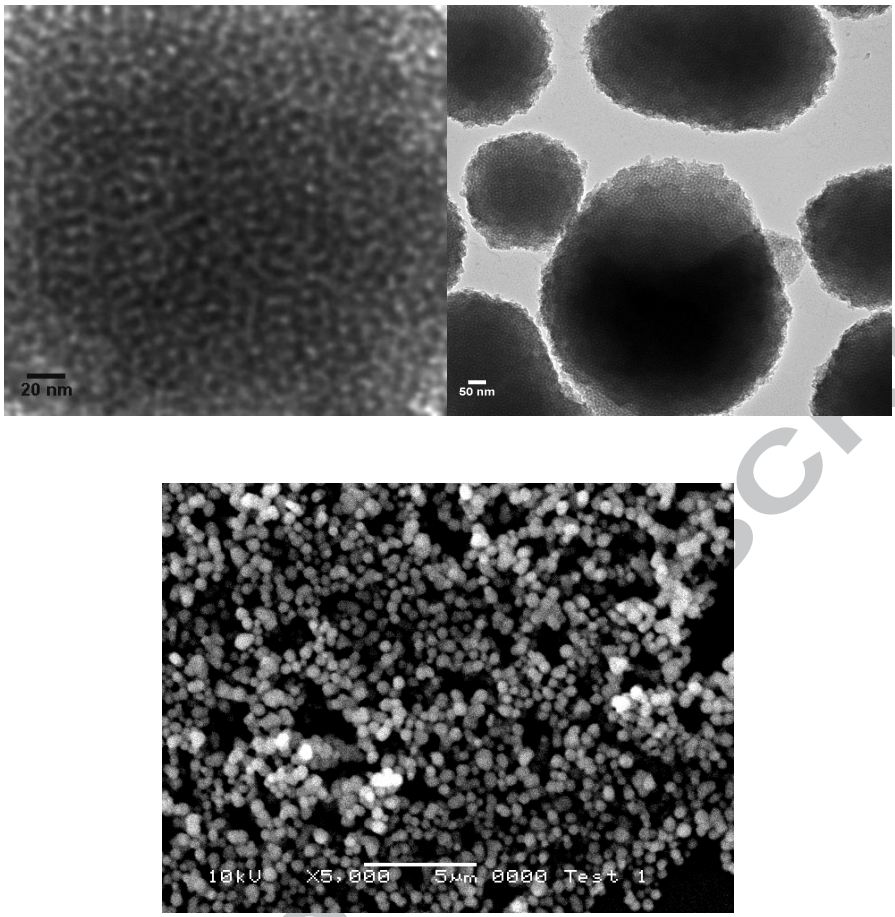


**Figure 6.** Upper: Transmission electron micrographs of a P123-F127 derived mesoporous silica calcined at 500 °C. The view along the [110] direction (left) and the bright field image of the mesoporous microspheres (right). Lower: Scanning electron micrographs of mesoporous microspheres of similar materials.

### *3.2. $V_2$-type surfactant*

***a) $V_2$-$V_1$ and $V_2$-$\nabla$ co-surfactants:*** Figure 7 shows the XRD data of mesoporous silica templated using F127 in combination with P65, L121 and 25R4 co-surfactant systems. For the F127-P65 and F127-25R4 systems only one broad low angle feature can be seen typical of a highly disordered mesoporous system. For F127-L121 there is only very weak x-ray scattering at low angles suggesting an almost amorphous silica structure is formed with little indication of pore ordering. The low angle diffraction peaks for these systems appear at $2\theta$ values of 0.93, 0.77 and 1.1° for F127-P65, -L121 and -25R4 surfactant mixtures respectively which correspond to *d*-spacings of 94.9, 114.6 and 80.2 Å. The $N_2$ sorption isotherms (Figure 7) of such materials are all type IV but with limited hysteresis compared to the data described above.

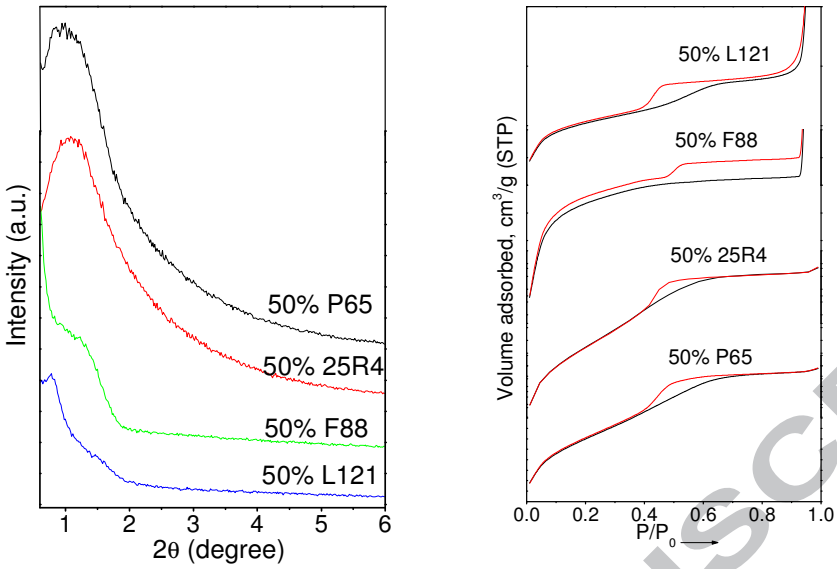


**Figure 7.** Powder XRD patterns (left) and $N_2$ adsorption isotherms (right) of mesoporous silicas (after calcination at 500 °C) derived from Pluronic F127-and other copolymer surfactants in equimolar amounts.

***b) $V_2$-$V_2$ co-surfactants.*** The XRD data from the F127-F88 derived mesoporous silica sample is unusual and indicates two types of pores are present. There is a poorly resolved reflection at $2\theta$ of 0.90° (Figure 7) with a steeply rising background at very low angle indicating the presence of pores > 12 Å in size. TEM revealed the presence of disordered pore systems and the $N_2$ sorption isotherms (Figure 7) was of an unusual shape. It could be categorized as type IV with a very wide hysteresis but the shape at the extremes of the $P/P_0$ range might indicate a significant micropore contribution. No clear PSD data could be obtained with a pore size distribution from around 2 – 15 nm indicated. The data appear to indicate that some large pores are formed, possibly from mixing of the surfactants to form large micellar structures, in combination with a highly disordered micropore and smaller mesopore structure (similar to that shown in Figure 1D).

Support for these suggestions can be gained from a study of varying co-surfactant concentration as shown in Figure 8. A pure F127 surfactant gives two fairly well resolved features (largest at about 1.25° 2θ) typical of a cubic mesopore system. F88 gives a broad feature (around 1.75° 2θ typical of a poorly ordered mesoporous system. Mixing the two surfactants gives an F88 type structure through the whole of the composition range with the position and shape of low angle XRD pattern being closely related to that of the F88 pattern. This would suggest that the F127 is partly

soluble in F88 and forming a range of mixed micelles. Around an equimolar concentration of the two surfactants it is clear that maximum disorder in the mesopores system is present in the system, as described above, as might be expected.

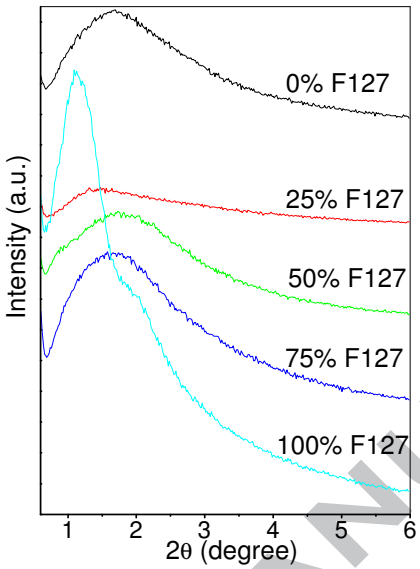


**Figure 8.** Powder X-ray diffraction patterns of the silica products derived from Pluronic F127 and F88 with different compositions calcined at 500 °C.

### *3.3. I-type surfactant*

***a) I-V and I-∇co-surfactants:*** Mesoporous silica made from equimolar amounts of I-type surfactants, e.g. B76 and V or ∇-type copolymer surfactants yielded only amorphous silica with no sign of any ordered mesoporosity as indicated by XRD or TEM. Of all the V or ∇ surfactants, only the B76-L121 system gives rise to a diffraction feature as shown in Figure 9. The feature is broad and there are no higher order reflections suggesting a disordered system with a range of pore sizes is present. It is interesting to note that the position of the peak is at relatively low angle (1.5° 2θ) typical of larger pore systems. There are no features > 2° 2θ typical of the low molecular weight Brij surfactants (see below). This may suggest that the Brij surfactant has formed mixed micelles with the L121 Pluronic. Additional evidence for this may be gained from examining different compositions. XRD shows the dramatic improvement of the order of such materials with the increasing of the relative molar content of B76 (0.95:0.5 mole fraction to the other surfactant) as described in Figure 10. In this figure it can be seen that reasonably well-ordered mesoporous systems are obtained for B76 in combination with P123 and 25R4. The B76–F127 is significantly less ordered than these with no well-resolved feature observed. It can be seen in the

data that the diffraction peak shifts to lower angle, higher d-spacing, as the molecular weight of the co-surfactant increases (molecular weight F127>P123>25R4). This would suggest that at these concentrations the co-surfactants are soluble in the B76 causing an expansion of the micelle size. This assumes that the d-spacing is closely related to the pore size. The relationship of the co-surfactant molecular weight to pore size is similar to that of Zhang [40] and Mou [41] *et al* who demonstrated the decrease in the pore diameter with the increase of the molar content of I-type ionic surfactants.

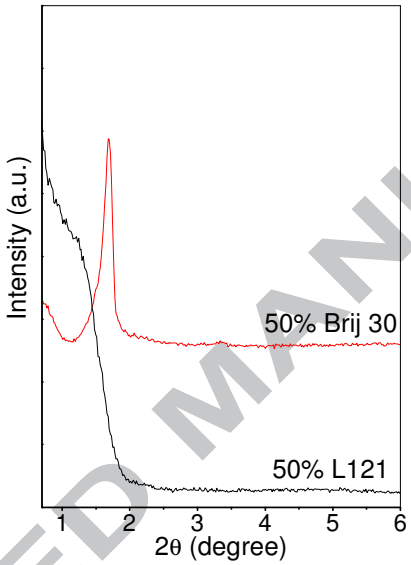


**Figure 9.** XRD patterns of mesoporous silicas derived from B76-B30 and B76-L121 equimolar surfactant concentrations.

***b) $I_1$-$I_2$ co-surfactants:*** Highly ordered monomodal mesoporous silicas were produced (as Figure 1A) by use of B76 and B30 as co-surfactant templates. XRD, Figure 9, shows a well-resolved high intensity feature on a low background typical of highly ordered materials. The XRD is similar to that reported of SBA-11 [8]. The $N_2$ adsorption-desorption isotherm (Figure 11) is type IV without hysteresis and shows a well-defined step in both the adsorption and desorption curves (essentially similar) between partial pressures $P/P_o$ of 0.2~0.4 (it should be noted that nitrogen adsorption isotherms will not reveal hysteresis in this range). BJH calculation give an average pore size of 22.2 Å (from adsorption and desorption branches of the isotherm). The width of the PSD at 5 Å (Figure 11) also indicates the formation of well-defined uniform pore dimensions. It is similar to that observed for mesoporous silica prepared

with a pure B76 surfactant phase [8] and it can be concluded that these similar surfactants form mixed micelles.

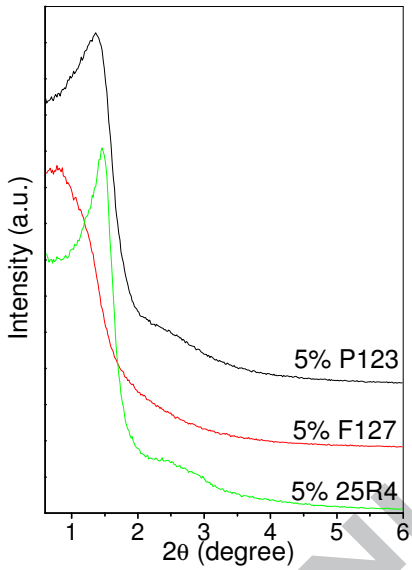


**Figure 10.** XRD patterns of mesoporous silicas derived from B76-P123, B76-F127 and B76-25R4 surfactant mixtures at a mole fraction of 0.95:0.05 Brij:co-surfactant.

### *3.4. X-type surfactant*

***a) X-V and X-∇co-surfactants:*** The combination of Tetronic 90R4 and Pluronic P123 can result in the formation of well-ordered mesoporous silica, ORK-4, as shown in Figure 12. Three well-resolved reflections typical of a hexagonal arrangement of pores are observed and can be indexed as (100), (110) and (200) reflections. The $d_{100}$ value is 113.2 Å and a unit cell parameter of 130.7 Å is estimated. This is significantly larger than that made from the single pure P123 copolymer [8] and data given in Figure 2 for other surfactant mixtures. In the presence of any other surfactants, the preparations yielded only amorphous silica with little sign of pore ordering. The observation of ordered XRD patterns and expansion of the usual P123 lattice parameters suggests some solubility of the 90R4 in the Pluronic and the system may be categorized as being similar to Figure 1A. This lattice expansion may be analogous to that measured for the additions of 1,3,5-trimethylbenzene (TMB) in SBA-15 systems [2] where the additive expands the micelle size.

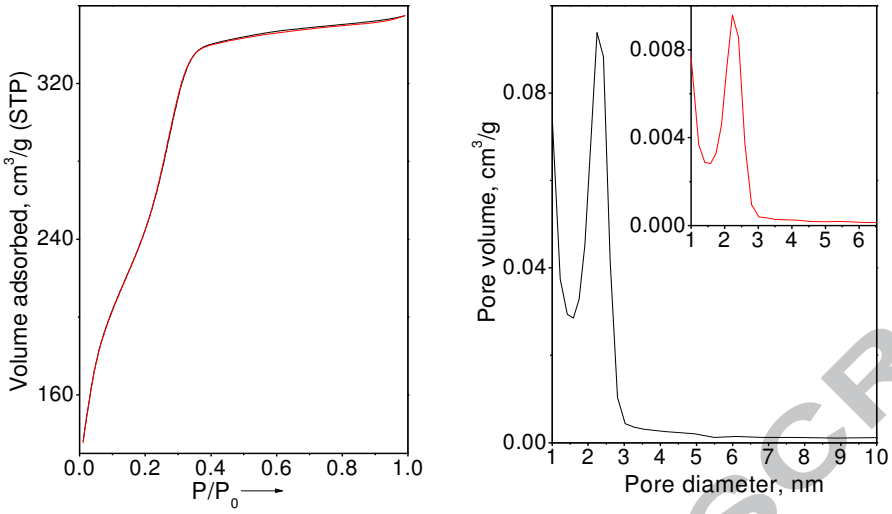


**Figure 11.** Left: $N_2$ adsorption-desorption isotherm of a mesoporous silica (calcined at 500 °C) templated by a equimolar mixture of B76 and B30. Right: corresponding pore-size distribution (PSD) curves determined by BJH analysis on the adsorption branch (right) and the desorption branch (inset) of the isotherms.

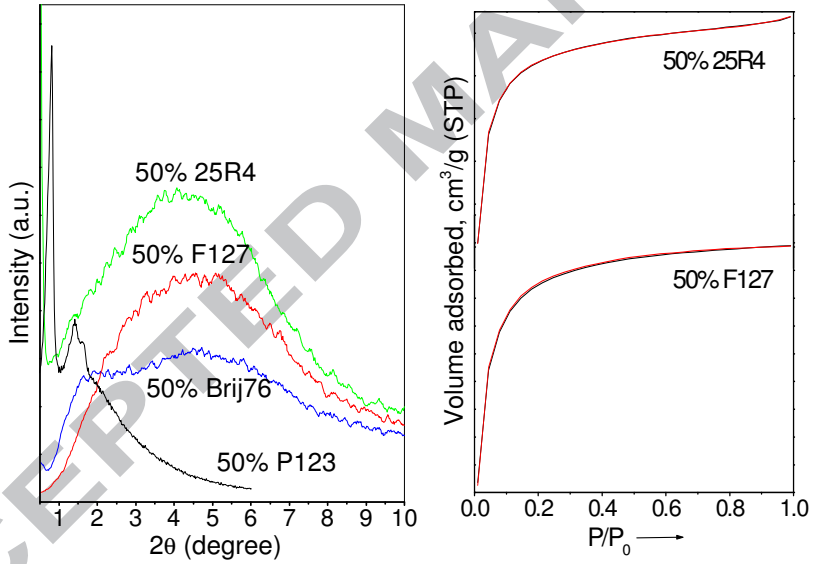


**Figure 12.** Left: powder x-ray diffraction patterns mesoporous silica (calcined at 500 °C) from mixed surfactants of Tetronic 90R4-derived with a equimolar concentration of other copolymers (see figure). Right: $N_2$ isotherm data from two of the samples as indicated in the figure.

The $N_2$ sorption isotherm (Figure 12) of ORK-4 is type IV with significant hysteresis. The desorption branch shows an intermediate step at around $P/P_0 = 0.6$ which is almost completely absent in the adsorption branch and as a result the BJH calculated pore size distribution is quite different for both (Figure 12). This suggests that the pores have a non-simple structure with some form of bimodal pore size

distribution. From both the XRD and isotherm data it can be concluded that the structure is as Fig 1B with the surfactants mixing to form regular micelle structures.

The other X-∇ combination, 90R4-F127, gave a very different result to the 90R4-P123 system displaying an XRD pattern with a very broad feature (Figure 12) at a 2$\theta$ position between 3~7° with a peak maximum corresponding to a *d*-spacing of 17.7 Å. The $N_2$ adsorption isotherm (Figure 12) of the same material has a type I isotherm typical of microporous solids [42, 43] and all evidence points to a microporous solid. It would appear that this surfactant system showed no tendency to mix and order was extremely limited as in Figure 1D.

The X-V combination, 90R4-25R4, gave very similar results to 90R4-F127 (Figure 12) and all evidence is of a disordered microporous material.

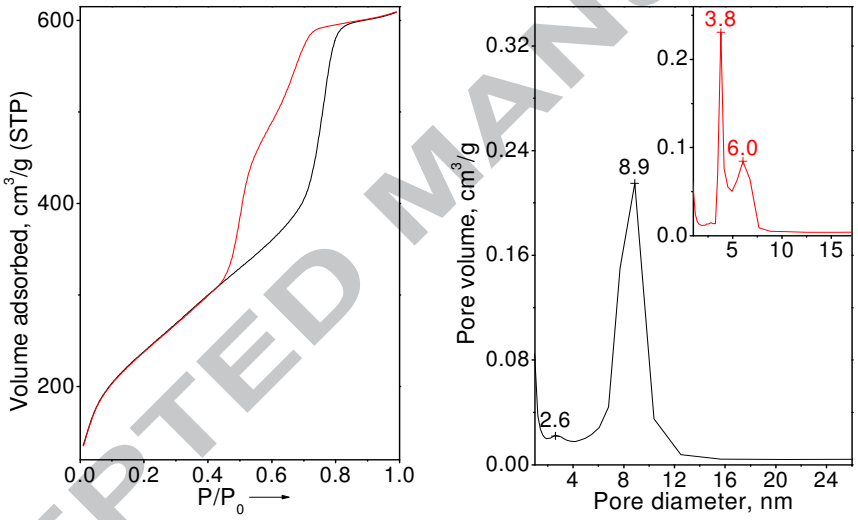


**Figure 12.** Nitrogen adsorption-desorption isotherms of 50 % of Tetronic 90R4 and 50 % P123 (co-)packed product calcined at 500 °C (left) and their corresponding pore-size distribution (PSD) curves determined by BJH analysis on the adsorption branch (right) and the desorption branch (inset) of the isotherms.

***b) X-I co-surfactants:*** The 90R4-B76 sample gave similar results to 90R4-F127 and 90R4-25R4. There is a very broad XRD feature at about 5° 2$\theta$ and the $N_2$ adsorption isotherm is largely typical of type I. There is some additional structure in the XRD pattern with a feature at about 2° 2$\theta$ and some hysteresis in the isotherm data. This might imply a mesoporous element of the porosity of this materials deriving from the B76 component and it can be concluded that the microporous behavior is typical of 90R4 templated pore systems and the mesoporous associated

with B76. It is also clear there is little tendency for the surfactants to form mixed micelles. The structure of the solid appears to resemble that described schematically in Figure 1C.

***c) $X_1$-$X_2$ co-surfactants:*** The Tetronic 701-90R4 co-surfactant mixture as a template for porous silica yield highly disordered microporous materials with poorly ordered structures as revealed by XRD.

### *3.5. Ternary co-surfactant*

Synthesis of a mesoporous silica from a complex surfactant mixture was also possible. Since P123 formed well ordered materials with P65 and 25R4 this V-V-V co-surfactant synthesis was carried out to produce ORK-5 (P123:25R4:P65=4:3:3 molar ratio). XRD (Figure 13) shows several clear diffraction peaks between 0.6 to 3°2$\theta$ for the calcined product that can be readily assigned to the same hexagonal mesoporous structure noted above for the P123-P65 and P123-25R4 mixtures. It should be noted that well-ordered porous structures are not present before calcination. The three XRD features correspond to the (100), (110) and (200) from a hexagonal *p6mm* unit cell. The cell parameter is 117.4 Å and is similar to the P123-P65 templated solid (ORK-1, 117.4 Å) and much larger than that derived from P123-25R4 pack system (ORK-2, 107.9 Å). The $N_2$ sorption isotherms (Figure 13) of ORK-5 are typical of type IV with strong hysteresis and the BJH calculation shows a bimodal PSD (Figure 13) in the desorption branch suggesting pore shape asymmetry in Figure 15. The width of the PSD of ~20 Å measured in the adsorption branch is also consistent with a varying pore diameter and the structure can be assigned to that of Figure 1B. Further evidence for this is provided by the TEM images presented in Figure 14. The micrographs show well-ordered hexagonal mesostructures viewed along the [001] and [110] directions, corresponding to the well-known hexagonal mesopore structures [2, 8]. The corresponding dark field image shows strong evidence for asymmetric pore shape and also a wide variation of pore size.

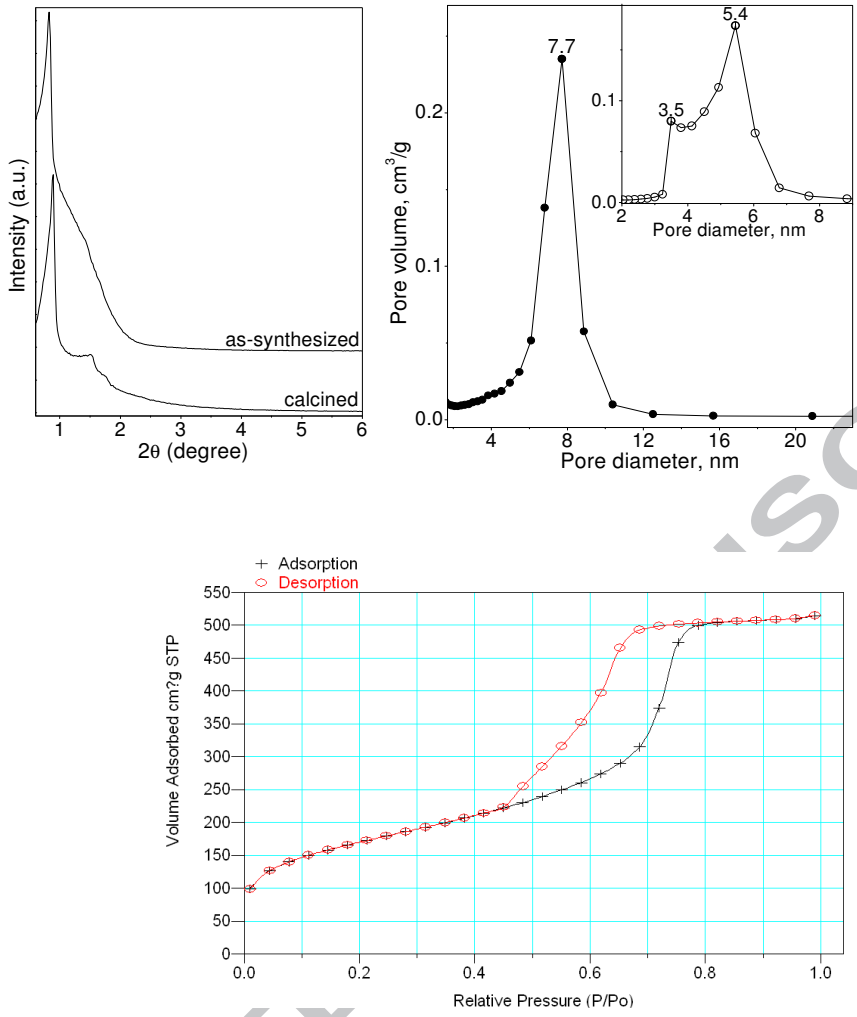


**Figure 13.** Upper left: PXRD of mesoporous silica synthesis via a ternary surfactant mixture of P123-P65-25R4 before and after calcination at 500 °C. Upper right: Corresponding pore-size distribution (PSD) curves determined by BJH analysis on the adsorption branch (right) and the desorption branch (inset) of the isotherms. Lower: Nitrogen adsorption-desorption isotherms of a 40% Pluronic P123, 30% P65 and 30% 25R4 product calcined at 500 °C.

Following this summary of the main systems and the behavior of co-surfactants as structural templates for porous silica formation, a simple means of understanding the behavior is provided below.

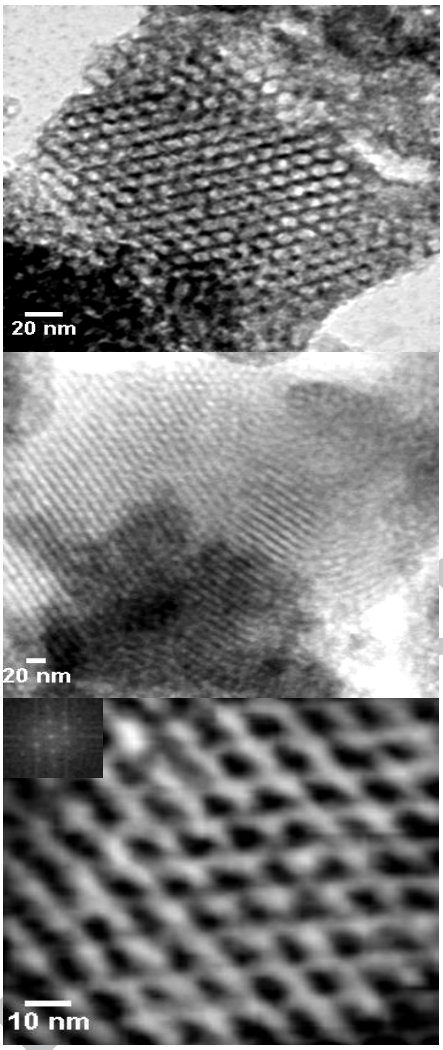


**Figure 14.** Transmission electron micrographs of the mesoporous silica templated from the P123-P65-25R4 ternary surfactant mixture after calcination: Top: view along the [001] direction; middle: the view along the [110] direction; bottom: the dark field view along the [001] direction its corresponding Fourier Transformation (inset) showing hexagonal symmetry.

## 4. Discussion

The data presented here show that the surfactant mixtures have provided a template for the formation of pores. However, it was found that the range of structural arrangements formed was large, from highly long range ordered systems to essentially amorphous porous silica. Providing a clear understanding of how these structures arise is difficult and reliant on two important processes. Firstly, the interaction of surfactants with each other and within the solvent to form mixed or non-mixed micelles and secondly, the ability of the micelles to pack into ordered micellar

arrangements. This latter point has been the subject of much research since the preparations used here are based on the widely-accepted cooperative self-assembly mechanism where it is only on interaction with the inorganic condensate that the micelles form these ordered arrangements and prior to this the templating micelles are subject to kinetically controlled association/dissociation equilibrium and Brownian motion [44]. Understanding how these surfactant mixtures might pack into ordered assemblies requires very extensive analysis and is beyond the scope of this article but will be discussed in depth elsewhere.

It is, however, rather simpler to provide a framework for understanding the possible interaction of the surfactant molecules (and, hence, how pore sizes and pore structures can be engineered by surfactant mixing) by comparing their chemical similarity. It is possible to define three conditions. Firstly, the surfactants are chemically similar and form micelles that are intimate mixtures with a uniform distribution of the surfactant molecules. Secondly, they are chemically dissimilar and the surfactants form individual micelle structures (or no micelles at all) and, thirdly, an intermediate interaction where micelles contain both surfactants but are regionalized to minimise any repulsive forces between the surfactant molecules. One can postulate that in closely similar surfactants a regular porous structure with uniformly sized pores may result (Figure 1A). In systems that form irregular mixed micelles than bimodal distributions may occur (Figure 1B). The non-interacting systems might form disordered or partially ordered structures such as Figure 1C and Figure 1D. Using this simple concept it can be understood why B30 and B76 form such a well ordered material. However, it is difficult to explain why two Pluronics, e.g. P123-F127 give such a poorly ordered material. To enable some deeper understanding a more quantitative explanation is required.

The cohesive energy, $E_{coh,}$ of a substance is a measure of the interaction between molecules in a condensed environment and is strictly defined as the increase in internal energy, U, per mole of substance if all of the intermolecular forces with its environment are eliminated. The $E_{coh}$ can be expressed as the cohesive energy (molar volume) density (ECD) = $E_{coh}/V_m$. Hildebrand [45-47] proposed that substances with similar cohesive energies should be soluble in one another, since, their internal energy would be little changed by mixing. In systems where the $E_{coh}$ was markedly different the substances would not mix since both internal energies would be increased. Hildebrand used a term known as the solubility parameter (or cohesion parameter for

a solid), $\delta = \sqrt{ECD}$, to define the probability of solution of one material in another. Solubility parameters can be used to predict the solubility of one component in another particularly through consideration of $\delta_A^2 - \delta_B^2$. If this is close to zero it implies that the molar enthalpies of vaporisation are similar and the intermolecular forces holding the components in a fluid or solid state similar. For example, if we take two polymers such that $\delta_A^2 - \delta_B^2$ has a significant magnitude then it would be expected that they would phase separate on mixing. It has further been shown for block copolymer (BCP) mixtures that an interaction parameter, $\chi$ can be written:

$$\chi = V_m(\delta_A - \delta_B)^2/RT \qquad \text{Eq.(1)}$$

where $V_m$ is the molar free volume (for mixing of two BCPs the average molar free volume) [48]. The use of this theory to understand mixing and phase separation has been reviewed by Morris et al [49]. Whilst a full description of this theory as applied to BCPs in solution is complex and beyond the scope of this paper, as a first approximation the effect of the solvent can be assumed to be minor. This is because, in Eq.(1), the difference between the solubility factor of water (~40 $MPa^{1/2}$) is very significantly greater than any of the BCPs used (16-25 $MPa^{1/2}$) and of course the reason why the BCPS generally form micelles (above their critical micelle concentration). Using known values of the interaction parameters and the properties of the individual BCPs (Table 1) as detailed elsewhere [46, 50] a table describing $\chi$ for each of the mixtures studied can be drawn up (Table 2). Since solvent parameters for all of the surfactants is not known, in this table it has been necessary to estimate the BCP surfactant solvent parameters: $s_{surfactant}$, from the solvent parameters of each block type, $\delta_{block\ A}$ and $\beta\delta_{block\ B}$, as: $s_{surfactant} = \alpha\delta_{block\ A} + \beta\delta_{block\ B}$ where $\alpha$ and $\beta$ are the fractions of each mer present in the surfactant. The following values were used; $\delta_{PE}$ = 16.2, $\delta_{PEO}$ = 24.2 and $\delta_{PPO}$ = 19.1 $MPa^{1/2}$.

In block copolymer theory, to describe the interactions between blocks and the microphase separation that results from these interactions, $\chi N$ (where N = degree of polymerisation and $\chi N$ can be described as the total interaction parameter) is used to provide an estimate of the total chemical interaction. In this theory for BCPs with equivalent block lengths, three regions are identified for phase separation. The first is the weak segregation (or separation) range, $10.5 \leq \chi N \leq 12.5$. Below $\chi N$ the interaction between blocks is not sufficient to cause ordered microphase separation. It should be noted that this minimum value of total interaction parameter increases as

composition varies from an equal mixture of components. The intermediate segregation limit is $12.5 \leq \chi N \leq 95$ and the strong segregation limit is defined by $\chi N \geq 100$ [49]. We can use this same approach to define regimes where the BCP surfactants in mesoporous silica formation used here can freely, partially or not mix during synthesis. If $\chi N$ is less than about 10 than the two BCP surfactants are chemically similar and will freely mix and form mixed micelle domains yielding mesoporous silica with mono-dispersed pore size distributions. If $10<\chi N<100$ (intermediate segregation) the surfactants will tend to phase separate but may form mesoporous silica with ordered arrangements of bimodal pore size distributions provided that at least one of the surfactants form these structures. If $\chi N$ is greater than about 100 (strong segregation), then disordered structures will be formed. These values can only be used as a guide because observation of well ordered mesoporous structures is also dependent on the ability of at least one of the surfactants to form ordered micelle arrangements that template mesoporous structures (as defined by packing ability).

This framework allows some interpretation of the data presented here to be made. In the case of the systems templated by mixing P123 with F127, L121, P65 and 25R4 the mesoporous material formed can be understood in terms of the value of $\chi N$ as given in Table 2. The P123-P65 and P123-P65 systems can be ascribed to intermediate values of $\chi N$ (P123-P65 is somewhat above the nominal value of 100 but ordering is probably driven by the strong tendency of both these surfactants to form highly ordered arrangements) and it can be expected that whilst there is little tendency for surfactants to form mixtures, their interaction energy is not sufficient to prevent ordering of the system. However, a $\chi N$ value of 358 for the P123-L121 system is too high for very well ordered arrangements and disorder is apparent from the XRD profiles. For P123-F127, the $\chi N$ value is so high that a well-ordered arrangement is not possible.

The mesoporous materials templated using F127 mixtures show little sign of forming well ordered mesopore arrangements. Less well-ordered arrangements may be expected because F127, Figure 8, does not form highly ordered arrangements in the absence of any other surfactants in these synthesis conditions. If mixed with surfactants that form well ordered structures it might be expected that the degree of ordering would be increased. However, mixing with P65, 25R4, F88 and L121 gave

highly disordered mesoporous/microporous arrangements and this would be predicted by the large $\chi N$ values in Table 2 and it is clear that there is little tendency for the surfactants to form mixed micelles and produce ordered materials.

The Brij surfactants are the most hydrophobic of the BCPs used here and only L121 and T701 are reasonably close in solubility value to these. As might be expected, mixing of B76 with the Pluronic systems gave highly disorganized materials. The only system to show any indication of mesoporosity was the B76-L121 system which has a $\chi N$ value indicating good mixing might be achieved. However, L121, in these conditions is known to form a thermally unstable lamellar phase [2, 8] and it is expected that the smaller Brij surfactant would not change the nature of the final silica product. The absence of any small mesopores does suggest that mixing of the surfactant was achieved. Whilst no ordered mesoporous silica was obtained from equimolar mixing of surfactants, evidence for some mixed micelle formation was obtained by preparing mixtures with lower secondary surfactant content (5 mole%). Since the $\chi$ value is dependent on concentration through the molar volume term, lower concentrations will yield lower $\chi N$ values as shown in Table 2. In this way, B76-P123 and B76-25R4 at these lower concentrations show resolved diffraction features (Figure 10) consistent with intermediate values of $\chi N$. Even at low concentrations F127 does not form good mixed micelles and no well-resolved XRD feature is observable. As would be suggested from the data in Table 2 where a low $\chi N$ value is seen, B76-B30 mixtures form a highly ordered hexagonal arrangement of pores with a monomodal pore size distribution and d-spacings and pore sizes intermediate between the two surfactants.

The complicated micelle structures 90R4, T701 and 25R4 are not known to form well ordered mesoporous structures except in thin films [51] and these are more often used to define particle morphologies rather than porosity. Thus, although 90R4-25R4 mixtures have a low $\chi N$ value, it is highly unlikely that an ordered structure could be formed even if well mixed micelles are observed. This is indeed case and in the system, as in most of the 90R4 systems studied, the result is a disordered microporous system. In all the other cases, with the exception of 90R4-P123, the $\chi N$ values would suggest strong segregation and non-mixing of the surfactants. The products of the 90R4-F127, 90R4-B76 and 90R4-T701 surfactant mixtures all appear to form disordered microporous systems consistent with molecular (rather than micelle) templating. The only system to show significant mesopores formation was 90R4-

P123 with a $\chi N$ value of 53 indicating intermediate segregation. The XRD and BET data are consistent with a well-ordered hexagonally packed mesopore system and data suggest some mixing of the surfactants within a bimodal distribution of pores.

Finally, the tertiary system, P123-25R4-P65, showed a well-ordered hexagonal arrangement of mesopores. Considering the mixture as a combination of 25R4-P123 and 25R4-P65 (Table 2) shows intermediate segregation with relatively low $\chi N$ values. Thus, even in complex systems, this solvent parameter model for predicting ordered mesopore structure formation appears to have value.

## 4. Conclusion

A series of mesoporous silicas were prepared using mixtures of block copolymer surfactants as templates. A range of structures, from highly ordered uniform pore sized arrangements through partially ordered complex bimodal structures and totally disordered non-mesoporous structures were observed. It is clear from the data presented here that formation of ordered mesoporous structures from surfactant mixtures is reliant on two factors; firstly, that at least one of the surfactants in the mixture forming ordered micellar structures in solution (in the presence of the silica precursor) and, secondly, that the surfactants are chemically not too different. In this paper we report that the solubility parameter defined total interaction parameter (essentially the cohesive energy multiplied by the degree of polymerization) provides a suitable means of predicting whether the surfactants will mix and hence form well-ordered mesoporous structures. The work is important in not only understanding the complex arrangements possible but also in allowing suitable systems to be chosen for pore size engineering of this important class of materials.

## Acknowledgment

We thank BASF (Mount Oliver, New Jersey, USA) for providing the block copolymer surfactants. We also acknowledge SFI (Science Foundation of Ireland) through the BIONANOINTERACT SRC Grant 07/SRC/B1155 and the SFI CRANN CSET grant which supported this work.

**References**

[1] D.H. Chen, Z. Li, C.Z. Yu, Y.F. Shi, Z.D. Zhang, B. Tu, D.Y. Zhao, Chem. Mater. 17 (2005) 3228.
[2] D.Y. Zhao, J.L. Feng, Q.S. Huo, N. Melosh, G.H. Fredrickson, B.F. Chmelka, G.D. Stucky, Science 279 (1998) 548.
[3] P.D. Yang, T. Deng, D.Y. Zhao, P.Y. Feng, D. Pine, B.F. Chmelka, G.M. Whitesides, G.D. Stucky, Science 282 (1998) 2244.
[4] M. Groenewolt, M. Antonietti, S. Polarz, Langmuir 20 (2004) 7811.
[5] P.D. Yang, D.Y. Zhao, D.I. Margolese, B.F. Chmelka, G.D. Stucky, Chem. Mater. 11 (1999) 2813.
[6] G.J.D.A. Soler-Illia, E.L. Crepaldi, D. Grosso, C. Sanchez, Curr. Opin. Colloid Interface Sci. 8 (2003) 109.
[7] D.Y. Zhao, B.Z. Tian, X.Y. Liu, Stud. Surf. Sci. Catal. 148 (2004) 139.
[8] D.Y. Zhao, Q.S. Huo, J.L. Feng, B.F. Chmelka, G.D. Stucky, J. Am. Chem. Soc. 120 (1998) 6024.
[9] B.G. Park, N.J. Jo, W.J. Cho, C.S. Ha, Polym. Int. 51 (2002) 1225.
[10] S.A. Bagshaw, E. Prouzet, T.J. Pinnavaia, Science 269 (1995) 1242.
[11] P.T. Tanev, T.J. Pinnavaia, Science 267 (1995) 865.
[12] S.A. Bagshaw, T.J. Pinnavaia, Angew. Chem. Int. Ed. 35 (1996) 1102.
[13] E. Prouzet, T.J. Pinnavaia, Angew. Chem. Int. Ed. 36 (1997) 516.
[14] G.S. Attard, J.C. Glyde, C.G. Goltner, Nature 378 (1995) 366.
[15] M.G. Song, J.Y. Kim, S.H. Cho, J.D. Kim, Langmuir 18 (2002) 6110.
[16] J.L. Shi, Z.L. Hua, L.X. Zhang, J. Mater. Chem. 14 (2004) 795.
[17] B. Smarsly, D. Grosso, T. Brezesinski, N. Pinna, C. Boissiere, M. Antonietti, C. Sanchez, Chem. Mater. 16 (2004) 2948.
[18] L. Sierra, S. Valange, J. Barrault, J.L. Guth, Micropor. Mesopor. Mater. 113 (2008) 352.
[19] E. Bloch, T. Phan, D. Bertin, P. Llewellyn, V. Hornebecq, Micropor. Mesopor. Mater. 112 (2008) 612.
[20] K.M. Ryan, N.R.B. Coleman, D.M. Lyons, J.P. Hanrahan, T.R. Spalding, M.A. Morris, D.C. Steytler, R.K. Heenan, J.D. Holmes, Langmuir 18 (2002) 4996.
[21] B.Z. Tian, X.Y. Liu, Z.D. Zhang, B. Tu, D.Y. Zhao, J. Solid State Chem. 167 (2002) 324.
[22] T.W. Kim, R. Ryoo, M. Kruk, K.P. Gierszal, M. Jaroniec, S. Kamiya, O. Terasaki, J. Phys. Chem. B 108 (2004) 11480.
[23] B.T. Holland, L. Abrams, A. Stein, J. Am. Chem. Soc. 121 (1999) 4308.
[24] L.M. Huang, Z.B. Wang, J.Y. Sun, L. Miao, Q.Z. Li, Y.S. Yan, D.Y. Zhao, J. Am. Chem. Soc. 122 (2000) 3530.
[25] C.J.H. Jacobsen, C. Madsen, J. Houzvicka, I. Schmidt, A. Carlsson, J. Am. Chem. Soc. 122 (2000) 7116.
[26] H. Mori, M. Uota, D. Fujikawa, T. Yoshimura, T. Kuwahara, G. Sakai, T. Kijima, Micropor. Mesopor. Mater. 91 (2006) 172.
[27] X.Z. Wang, T. Dou, Y.Z. Xiao, Chem. Commun. (1998) 1035.
[28] S.A. Bagshaw, Chem. Commun. (1999) 1785.
[29] J.H. Sun, Z.P. Shan, T. Maschmeyer, M.O. Coppens, Langmuir 19 (2003) 8395.
[30] J.H. Sun, Z.P. Shan, T. Maschmeyer, J.A. Moulijn, M.O. Coppens, Chem. Commun. (2001) 2670.

[31] J. El Haskouri, D.O. de Zarate, C. Guillem, J. Latorre, M. Caldes, A. Beltran, D. Beltran, A.B. Descalzo, G. Rodriguez-Lopez, R. Martinez-Manez, M.D. Marcos, P. Amoros, Chem. Commun. (2002) 330.
[32] Z.Y. Yuan, J.L. Blin, B.L. Su, Chem. Commun. (2002) 504.
[33] K. Ikari, K. Suzuki, H. Imai, Langmuir 20 (2004) 11504.
[34] D.B. Kuang, T. Brezesinski, B. Smarsly, J. Am. Chem. Soc. 126 (2004) 10534.
[35] O. Sel, D.B. Kuang, M. Thommes, B. Smarsly, Langmuir 22 (2006) 2311.
[36] J.M. Kim, Y. Sakamoto, Y.K. Hwang, Y.U. Kwon, O. Terasaki, S.E. Park, G.D. Stucky, J. Phys. Chem. B 106 (2002) 2552.
[37] L. Chen, W.H. Zhang, J. Xu, D.A. Tanner, M.A. Morris, Micropor. Mesopor. Mater. 129 (2010) 179.
[38] D.Y. Zhao, J.Y. Sun, Q.Z. Li, G.D. Stucky, Chem. Mater. 12 (2000) 275.
[39] J.P. Hanrahan, A. Donovan, M.A. Morris, J.D. Holmes, J. Mater. Chem. 17 (2007) 3881.
[40] W.H. Zhang, L. Zhang, J.H. Xiu, Z.Q. Shen, Y. Li, P.L. Ying, C. Li, Micropor. Mesopor. Mater. 89 (2006) 179.
[41] B.C. Chen, M.C. Chao, H.P. Lin, C.Y. Mou, Micropor. Mesopor. Mater. 81 (2005) 241.
[42] F. Liebau, Micropor. Mesopor. Mater. 58 (2003) 15.
[43] L.B. McCusker, F. Liebau, G. Engelhardt, Micropor. Mesopor. Mater. 58 (2003) 3.
[44] R. Nagarajan, Langmuir 18 (2002) 31.
[45] J. Burke, Solubility Parameters : Theory and Application. The Oakland Museum of California, 1984.
[46] A.F.M. Barton, CRC handbook of polymer-liquid interaction parameters and solubility parameters. CRC Press, Boca Raton, 1990.
[47] J.H. Hildebrand, Solubility of non-electrolytes, Reinhold, New York, NY, 1936.
[48] F.S. Bates, Science 251 (1991) 898.
[49] R.A. Farrell, T.G. Fitzgerald, D. Borah, J.D. Holmes, M.A. Morris, Int. J. Mol. Sci. 10 (2009) 3671.
[50] J.I.E.H.G.E.A. Brandrup, Polymer handbook, Wiley-Interscience, New York ; Chichester, 1999.
[51] K. M. Ryan, W. Lawton; J. D. Holmes and M. A. Morris, US patent, US 6,699.797 B1, 2004.

**Table 1.** Physical properties of the block copolymer surfactants used in this study

| | B30 | B76 | L121 | P65 | P123 | F127 | F88 | 25R4 | T701 | 90R4 |
|---|---|---|---|---|---|---|---|---|---|---|
| Mol. Wt ($g\ mol^{-1}$) | 363 | 711 | 4400 | 3400 | 5750 | 12600 | 11400 | 3600 | 3700 | 6900 |
| Density ($g\ cm^{-3}$) | 0.946 | 0.965 | 1.01 | 1.05 | 1.01 | 1.05 | 1.06 | 1.05 | 1.02 | 1.05 |
| $V_m$ ($cm^3\ mol^{-1}$) | 384 | 737 | 4356 | 3238 | 5693 | 12000 | 10755 | 3429 | 3627 | 6571 |
| Sol. Para-meter $(MPA)^{1/2}$ | 18.2 | 19.05 | 19.37 | 22.02 | 20.95 | 22.93 | 23.37 | 21.47 | 19.27 | 21.43 |

**Table 2.** Calculation of $\chi$ for the surfactant mixtures used in the synthesis of mesoporous silica.

| Surfactant 1 | Surfactant 2 | $V_{m(ave)}/RT$ | $(\delta_1-\delta_2)^2$ | $\chi$ | $\chi N$ | Structure |
|---|---|---|---|---|---|---|
| P123 | F127 | 2.66 | 3.92 | 10.4 | 2044 | Ordered |
| | L121 | 1.51 | 2.50 | 3.8 | 358 | Some ordering, bimodal |
| | P65 | 1.34 | 1.14 | 1.5 | 139 | Good ordering, bimodal |
| | 25R4 | 1.37 | 0.27 | 0.37 | 33.5 | Good ordering, bimodal |
| | | | | | | |
| F127 | P65 | 2.29 | 0.83 | 1.9 | 334 | Disordered |
| | 25R4 | 2.32 | 2.13 | 4.9 | 873 | Disordered |
| | F88 | 3.42 | 0.19 | 0.66 | 172 | Disordered |
| | L121 | 2.46 | 12.67 | 31.2 | 5641 | Amorphous |
| | | | | | | |
| B76 | B30 | 0.17 | 0.72 | 0.12 | 2.7 | high order, monomodal |
| | L121 | 0.76 | 0.10 | 0.09 | 4.2 | Mixed, ordering? |
| | F127 | 0.39 | 15.05 | 5.9 | 912 | Disordered |
| | P123 | 0.29 | 3.61 | 1.1 | 73 | Some ordering |
| | 25R4 | 0.26 | 5.86 | 1.5 | 76 | Some ordering |
| | | | | | | |
| 90R4 | 25R4 | 1.50 | 0.02 | 0.00 | 0.25 | Microporous |
| | F127 | 2.79 | 2.25 | 6.3 | 1326 | Microporous |
| | B76 | 1.10 | 5.66 | 6.2 | 523 | Microporous |
| | P123 | 1.84 | 0.23 | 0.4 | 53 | Good ordering, bimodal |
| | T701 | 1.53 | 4.24 | 6.5 | 664 | Microporous |
| | | | | | | |
| 25R4 | P123 | 1.42 | 0.27 | 0.4 | 34.8 | Good ordering, bi |
| 25R4 | P65 | 1.00 | 0.29 | 0.3 | 20.6 | Good ordering, bi |

**Figure Captions**

**Figure 1.** Schematic represent for interstitial and substitutional pore configuration of the dual pore/bimodal mesoporous systems.

**Figure 2.** Powder x-ray diffraction patterns of Pluronic P123 (with an equimolar amount of other surfactants) derived mesoporous silica (after 500 °C calcination).

**Figure 3.** Transmission electron micrographs of a P123-P65 product calcined at 500 °C. Left is the view along the [001] direction and its corresponding Fourier Transformation (inset) and the view along the [110] direction (right).

**Figure 4.** Nitrogen adsorption-desorption isotherms of Pluronic P123-derived products calcined at 500 °C (left) and (right) their corresponding pore-size distribution (PSD) curves (determined by Barrett-Joyner-Halenda (BJH) analysis on desorption branches of the isotherms). Solid symbols denote the adsorption branches while the open symbols indicate the desorption branch.

**Figure 5.** Transmission electron micrographs of a mesoporous silica templated by a equimolar mixture of P123 and 25R4 following calcination at 500 °C. Left, the view along the [001] direction and its corresponding Fourier Transformation inset and the view along the [110] direction (right).

**Figure 6.** Upper: Transmission electron micrographs of a P123-F127 derived mesoporous silica calcined at 500 °C. The view along the [110] direction (left) and the bright field image of the mesoporous microspheres (right). Lower: Scanning electron micrographs of mesoporous microspheres of similar materials.

**Figure 7.** Powder XRD patterns (left) and $N_2$ adsorption isotherms (right) of mesoporous silicas (after calcination at 500 °C) derived from Pluronic F127-and other copolymer surfactants in equimolar amounts.

**Figure 8.** Powder X-ray diffraction patterns of the silica products derived from Pluronic F127 and F88 with different compositions calcined at 500 °C.

**Figure 9.** XRD patterns of mesoporous silicas derived from B76-B30 and B76-L121 equimolar surfactant concentrations.

**Figure 10.** XRD patterns of mesoporous silicas derived from B76-P123, B76-F127 and B76-25R4 surfactant mixtures at a mole fraction of 0.95:0.05 Brij:co-surfactant.

**Figure 11.** Left: $N_2$ adsorption-desorption isotherm of a mesoporous silica (calcined at 500 °C) templated by a equimolar mixture of B76 and B30. Right: corresponding

pore-size distribution (PSD) curves determined by BJH analysis on the adsorption branch (right) and the desorption branch (inset) of the isotherms.

**Figure 12.** Left: powder x-ray diffraction patterns mesoporous silica (calcined at 500 °C) from mixed surfactants of Tetronic 90R4-derived with a equimolar concentration of other copolymers (see figure). Right: $N_2$ isotherm data from two of the samples as indicated in the figure.

**Figure 13.** Upper left: PXRD of mesoporous silica synthesis via a ternary surfactant mixture of P123-P65-25R4 before and after calcination at 500 °C. Upper right: Corresponding pore-size distribution (PSD) curves determined by BJH analysis on the adsorption branch (right) and the desorption branch (inset) of the isotherms. Lower: Nitrogen adsorption-desorption isotherms of a 40% Pluronic P123, 30% P65 and 30% 25R4 product calcined at 500 °C.

**Figure 14.** Transmission electron micrographs of the mesoporous silica templated from the P123-P65-25R4 ternary surfactant mixture after calcination: Top: view along the [001] direction; middle: the view along the [110] direction; bottom: the dark field view along the [001] direction its corresponding Fourier Transformation (inset) showing hexagonal symmetry.

'Syntheses of Complex Mesoporous Silicas Using Mixtures of Nonionic Block Copolymer Surfactants: Understanding Formation of Different Structures Using Solubility Parameters' is a story about the synthesis of ordered or disordered, bimodal/dual pore or mono-modal mesoporous silica by nonionic block copolymer (BCP) co-surfactants under mild conditions.

- Formation of ordered mesoporous structures via a range of surfactant mixtures rather than single surfactants;
- Formation of complex bi-modal pore size distributions in mesoporous materials via the different combination of two or three different types of surfactants;
- The use of solvent parameter theory to understand mesoporous structure formation in complex systems.